Journal of Pharmaceutical Analysis 16 (2026) 101335

Contents lists available at ScienceDirect

Journal of Pharmaceutical Analysis

journal homepage: www.elsevier.com/locate/jpa

Original article

# Screening of tyrosine phosphatase SHP2 (PTPN11) inhibitors from natural products with therapeutic potential for receptor tyrosine kinase-driven cancer

Lingfeng Chen [a, b, 1, **], Di Ke [c, 1], Zheng Jiang [a, 1], Ruixiang Luo [a], Jie Li [d], Lulu Zheng [e], Guang Liang [a, b, *]

[a] School of Pharmacy, Hangzhou Medical College, Hangzhou, 310014, China
[b] Department of Pharmacy and Institute of Inflammation, Zhejiang Provincial People's Hospital, Affiliated People's Hospital, Hangzhou Medical College, Hangzhou, 310014, China
[c] Institute of Health and Medicine, Hefei Comprehensive National Science Center, Hefei, 230601, China
[d] School of Medicine, Zhejiang University City College, Hangzhou, 310015, China
[e] Department of Pharmacy, Tongde Hospital of Zhejiang Province, Hangzhou, 310000, China

ARTICLE INFO

*Article history:*
Received 21 December 2024
Received in revised form
5 May 2025
Accepted 6 May 2025
Available online 9 May 2025

*Keywords:*
SHP2
High-throughput screening
Lead compound
Natural products
Allosteric inhibitor

ABSTRACT

Src homology 2 domain-containing phosphatase 2 (SHP2) is a pivotal regulator linking receptor tyrosine kinase (RTK) signaling. Abnormal SHP2 activity has been associated with tumorigenesis and metastasis. Although some SHP2-targeting modulators have entered clinical trials, U.S. Food and Drug Administration (FDA)-approved SHP2 targeting drugs are still not available. Herein, we describe cooperative biochemical inhibition experiments that facilitate the identification of both catalytic and allosteric SHP2 inhibitors using an in-house natural product (NP) library. Based on this screening methodology, structurally diverse sets of NPs were characterized, among which dihydrotanshinone I (DHT) potently inhibited the wild-type SHP2 protein tyrosine phosphatase (PTP) domain and gain-of-function SHP2 variants. Trichostatin A (TSA) bound to the "tunnel" binding site, acting as an allosteric inhibitor. This study illustrates an optimized screening methodology and tactics to identify novel SHP2 modulators from NPs and provides a foundation for further NP-based drug development for the treatment of RTK-driven cancer.


## 1. Introduction

Src homology 2 domain-containing phosphatase 2 (SHP2) (also known as PTPN11) is the first reported oncogenic protein tyrosine phosphatase (PTP) [1]. SHP2 is ubiquitously expressed in cells and functions as a signal adaptor for receptor tyrosine kinases (RTKs). SHP2 regulates oncogenic signaling by activating the mitogen-activated protein kinases (MAPKs), phosphoinositide 3-kinase (PI3K), and signal transducer and activator of transcription (STAT) cascades [2]. In addition, SHP2 contributes to immune evasion by participating in programmed cell death 1/programmed death ligand 1 (PD-1/PD-L1) signaling [3]. Gain-of-function mutations in SHP2 have been detected in severe diseases, such as LEOPARD and Noonan syndrome. The aberrant activation of SHP2 is prevalent in various cancer types, including leukemia and solid tumors [4]. Thus, SHP2 is an attractive therapeutic molecule for various diseases.

SHP2 belongs to the non-receptor PTP family and consists of a single PTP catalytic region, two SH2 structural domains, and a short C-tail (CT) comprising two tyrosine phosphorylation residues [5] (Figs. 1A and B). In its resting state, the N-SH2 moiety of SHP2 blocks the PTP catalytic site and restricts substrate entry into the catalytic pocket [5] (Fig. 1B). After the pTyr-containing substrate docks to N-SH2, the autoinhibited SHP2 is transformed into an activated conformation that exposes the catalytic site by disrupting the SH2-

This article is part of a special issue entitled: Targeted drug screening published in Journal of Pharmaceutical Analysis.

Peer review under responsibility of Xi'an Jiaotong University.

* Corresponding author. Department of Pharmacy and Institute of Inflammation, Zhejiang Provincial People's Hospital, Affiliated People's Hospital, Hangzhou Medical College, Hangzhou, 310014, China.
** Corresponding author. Department of Pharmacy and Institute of Inflammation, Zhejiang Provincial People's Hospital, Affiliated People's Hospital, Hangzhou Medical College, Hangzhou, 310014, China.
*E-mail addresses:* lfchen@hmc.edu.cn (L. Chen), 2020000411@hmc.edu.cn (G. Liang).

[1] These authors contributed equally to this work.

https://doi.org/10.1016/j.jpha.2025.101335

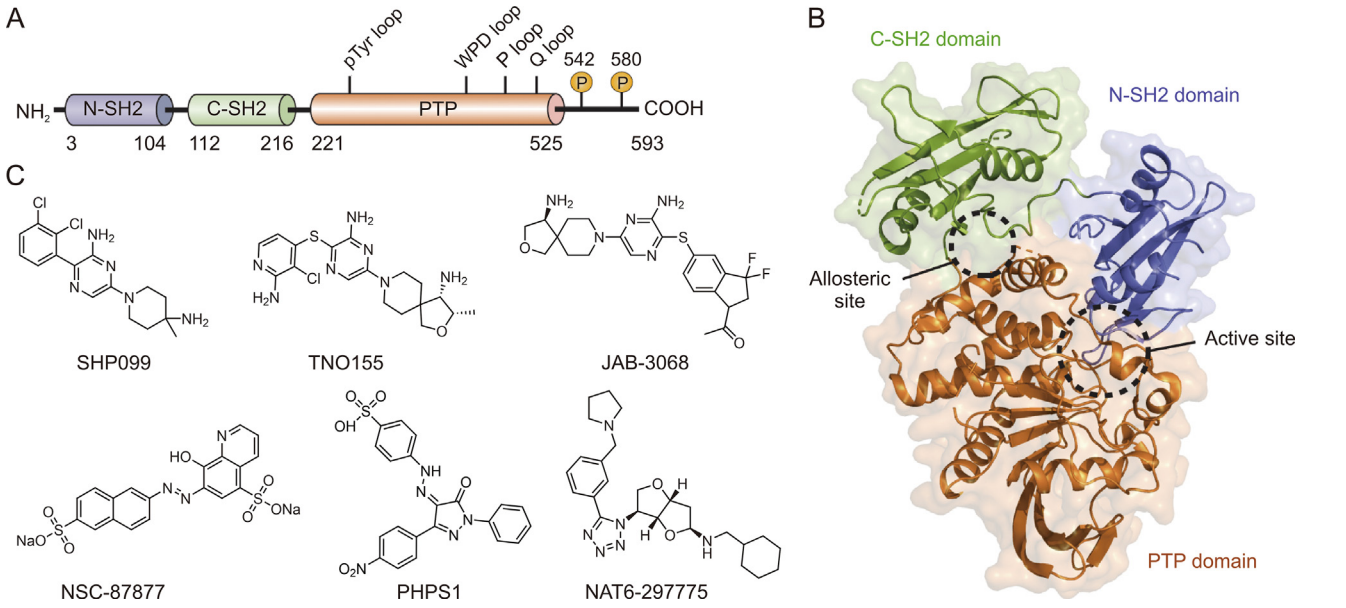


**Fig. 1.** Representative inhibitors targeting the allosteric sites and catalytic active site. (A) Schematic illustration of Src homology region 2-containing protein tyrosine phosphatase 2 (SHP2). (B) Crystal structure of the autoinhibited state SHP2 (Protein Data Bank (PDB) ID: 2SHP). The inhibitor binding site is highlighted with a circle. (C) Chemical structures of representative identified SHP2-targeted molecules. WPD: tryptophan (W), proline (P), and aspartate (D); PTP: protein tyrosine phosphatase.

PTP association [6]. Owing to the unique structure of SHP2, two types of small-molecule inhibitors have been reported (Figs. 1B and C).

Traditional SHP2 inhibitors interact specifically with the PTP domain and block its enzymatic activity, such as NSC-87877 [7], PHPS1 [8], and NAT6-297775 [9]. Most SHP2 allosteric inhibitors enter the tunnel drug-binding site created by the boundary between the SH2 and PTP domains, thereby stabilizing the inactive state of the enzyme. However, to date, no compounds have entered clinical trials [4]. SHP099 is an allosteric site inhibitor discovered by Novartis, which boosted the discovery of SHP2-targeted allosteric inhibitors [2]. To date, numerous SHP099-derived inhibitors, including TNO155 [10], JAB-3068 [11], RLY-1971 (GDC-1971) [12], and PF-07284892 (ARRY-558) [13] have advanced into different phases of clinical trials for cancer treatment. Despite tremendous progress achieved with SHP2 allosteric inhibitors, several SHP2 inhibitor treatments have shown limited benefits in patients [14]. In 2021, Novartis terminated a clinical trial of TNO155 because of its insufficient efficacy in the treatment of solid tumors (Trial No.: NCT03114319). Therefore, the discovery of novel SHP2 inhibitors with different molecular structures is clinically significant.

Natural products (NPs), along with their derivatives, have provided abundant candidates for the identification of novel chemical structures with a wide range of therapeutic activities and a great variety of scaffolds that can be lead compounds for modification or even direct use [15,16]. Thus, understanding the biological and molecular mechanisms of NPs has led to the identification of novel drugs for treating human diseases. NPs are a promising source of PTP inhibitors [17]. Many potent protein tyrosine phosphatase 1B (PTP1B) inhibitors have been developed from natural sources and have shown potential in the management of type 2 diabetes [18,19]. Few studies have also reported NPs or their derivatives as potential inhibitors of SHP2, including celastrol [20], tautomycetin [21], and cryptotanshinone [22]. However, the structure-activity relationship (SAR) or underlying inhibition mechanism of these NPs remains unclear. This study aimed to identify novel SHP2 inhibitors in NPs by establishing a new cross-validation drug screening paradigm based on the protocols reported by several other groups [2,23,24], leading to the identification of novel lead compounds and molecular skeletons for further drug development (Fig. 2).

## 2. Materials and methods

### 2.1. Protein expression and purification

Two human SHP2 constructs were created by cloning the *PTPN11* gene, which encodes the truncated forms A237-I529 (designated SHP2-PTP) and M1-L525 (designated SHP2-FL), into the pET30 vector by Beijing Tsingke Biotech Co., Ltd. (Beijing, China). The constructs were framed in-frame with a 6× His-tag to facilitate protein purification. Using these plasmids as templates, site-directed mutagenesis was performed to generate a series of mutants, including $SHP2^{E76K}$, $SHP2^{D61V}$, $SHP2^{T253M}$, $SHP2\text{-}PTP^{R465A}$, and $SHP2\text{-}PTP^{Q510A}$. The resulting constructs were introduced into BL21 (DE3) *Escherichia coli* (*E. coli*) cells. The bacterial cultures were grown to an optical density at 600 nm ($OD_{600}$) between 0.8 and 1.0, and SHP2 expression was induced overnight at 18 °C with 0.5–1 mM isopropyl-beta-D-thiogalactopyranoside (IPTG).

The cells were harvested and added to buffer consisting of 50 mM Tris-HCl (pH 8.5), 50 mM NaCl, 50 mM imidazole, and 5%–10% glycerol. The cells were then lysed and filtered. The supernatant was further diluted in lysis buffer. The mixture was loaded onto a 5 mL Ni-NTA gravity column (#88221; Thermo Fisher Scientific Inc., Fair Lawn, NJ, USA) and eluted with 200 mM imidazole. The eluted protein was diluted with 50 mM NaCl in 25 mM Tris-HCl buffer and applied to a HiTrap Q anion-exchange column (#17515601; GE Healthcare, Chicago, IL, USA). SHP2 bound to the column was eluted using a linear NaCl gradient (0–0.5 M) over 15 column volumes of the same buffer. Fractions containing SHP2 were purified using size-exclusion chromatography (Superdex 200; GE Healthcare) in 25 mM Tris-HCl (pH 8.5) and 150 mM NaCl buffer. The purified phosphatase proteins were then flash-frozen in liquid nitrogen and stored at −80 °C until further use. This procedure was also applied to purify the SHP2 mutants.

For other PTPs, complementary DNA (cDNA) fragments encoding residues M1–G305 of the human PTPN12 catalytic domain and full-length human low molecular weight protein tyrosine phosphatase (LMWPTP) (M1–H158) were amplified using polymerase chain reaction (PCR) and subsequently subcloned into the pET28a vector. Protein expression and purification were performed

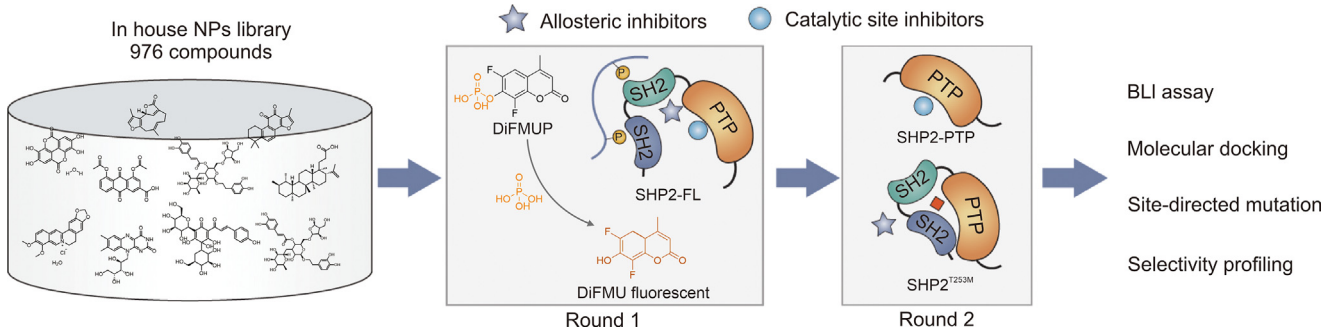


**Fig. 2.** Workflow of the complementary cross-validation drug screening paradigm. For the first-round screening, the assay was conducted using full length Src homology region 2-containing protein tyrosine phosphatase 2 (SHP2-FL); for second-round validation assay, active site inhibitors were validated using protein tyrosine phosphatase (PTP) domain of SHP2 protein. The allosteric inhibitors were tested against the site-mutated protein $SHP2^{T253M}$. Subsequently, hit compounds were further cross-validated via bio-layer interferometry (BLI) assay, molecular simulation, and site-directed mutagenesis studies. NPs: natural products; DiFMUP: 6,8-difluoro-4-methylumbellyferyl phosphate; DiFMU: 6,8-difluoro-7-hydroxy-4-methylcoumarin.

following the same protocol used for SHP2. Other PTPs, including PTP1B, PTP receptor type A (PTPRA), and PTP non-receptor type 6 (PTPN6), were purchased from Sino Biological (Shanghai, China).

### 2.2. SHP2 inhibition assay

The enzymatic activity of SHP2 was assessed using 6,8-difluoro-4-methylumbellyferyl phosphate (DiFMUP) (#D22065; Thermo Fisher Scientific Inc.), a surrogate tyrosine phosphatase substrate, using a fluorescence-based assay. Reactions were carried out at 20 °C in a 384-well plate (#781086; Greiner Bio-One, Monroe, NC, USA). The reaction buffer consisted of 60 mM 4-(2-hydroxyethyl)-1-piperazineethanesulfonic acid (HEPES) (pH 7.5), 75 mM NaCl, 75 mM KCl, 1 mM ethylenediamine tetraacetic acid (EDTA), 0.05% Tween-20, and 5 mM dithiothreitol.

Test NP libraries were collected from TargetMol Chemicals Inc. (Boston, MA, USA) and resuspended in dimethyl sulfoxide (DMSO) at a stock concentration of 10 mM. SHP2 enzyme and the test NPs were incubated in the presence of 0.5 μM of phosphorylated insulin receptor substrate 1 (p-IRS-1) peptide (sequence: LN(pY) IDLDLV(dPEG8)LST(pY)ASINFQ) synthesized by ChinaPeptides (Shanghai, China). After a 0.5 h-incubation at 25 °C, DiFMUP (10 μM) was added to the reaction, which was incubated at room temperature for another 0.5 h. Finally, the reaction was quenched by adding 50 μM solution of bpV(Phen) (#SML0889; MilliporeSigma, Darmstadt, Germany). Measurements were performed using a SpectraMax iD5 (Molecular Devices, LLC, San Jose, CA, USA) instrument with excitation and emission wavelengths of 340 and 450 nm, respectively. The allosteric compound TNO155 was used as a control for full length SHP2 (SHP2-FL) activity. Initial hits were selected that had an inhibition rate over 60% at a concentration of 20 μM. Initial hits were further cross-validated using an SHP2-PTP inhibition assay to confirm the binding sites of hit compounds.

### 2.3. Bio-layer interferometry (BLI) assay

Purified SHP2 was incubated with NHS-PEG12-Biotin in a 1:1.5 molar ratio for 1 h at room temperature. The biotin-labeled protein samples were loaded onto a gel column (#G-MM-IGT; Genemore, Suzhou, China) for purification. The biotinylated protein was bound to the super streptavidin (SSA) sensors. The kinetics of SHP2 binding to compounds were measured by immersing the sensors in a 96-well plate with various concentrations of compounds for 300 s, followed by dissociation in the same buffer devoid of SHP2 for an additional 300 s. The equilibrium dissociation constant ($K_D$) was determined using the FortéBio Octet 96 system (Sartorius Group, Göttingen, Germany).

### 2.4. Molecular modeling of the complex of trichostatin A (TSA) bound to SHP2

The initial binding sites between SHP2 and TSA were predicted using the Glide module of the Schrödinger package [25]. Grids for the "tunnel" and "latch" binding sites were generated using the module of Receptor Grid Generation. The Glide module was then employed to predict the potential binding positions between SHP2 and TSA. The most favorable binding poses of TSA at the "tunnel" and "latch" sites were subjected to molecular dynamics (MD) simulations. Three parallel 500 ns MD simulations were performed following procedures similar to those reported in previous studies [26,27]. The root mean square deviations (RMSDs) of SHP2 and TSA were calculated using the CPPTRAJ module in the Amber 18 package [28]. For per-residue decomposition, MD simulation trajectories from 400 to 500 ns were analyzed using 1000 snapshots each, based on the molecular mechanics/generalized born surface area (MM/GBSA) method, as previously described [29].

### 2.5. Cell culture and Western blotting

NCI-H1975 cells were cultured in Roswell Park Memorial Institute (RPMI) 1640 medium supplemented with 10% fetal bovine serum (FBS) (ExCell Bio, Taicang, China). Cell samples were lysed in radioimmunoprecipitation assay buffer (RIPA) buffer containing phosphatase and protease inhibitors. Protein samples were separated, transferred, and incubated overnight at 4 °C with target antibodies diluted in 5% bovine serum albumin (BSA). Antibodies were visualized using enhanced chemiluminescence reagents (NCM Biotech, Newport, RI, USA) on a Fusion FX system (Vilber, Collégien, France). Antibodies against phosphorylated extracellular signal-regulated kinase 1/2 (p-ERK1/2) (#4370), β-actin (#3700), and ERK (#4695) were purchased from Cell Signaling Technology (Danvers, MA, USA).

### 2.6. Colony formation assay and cell proliferation assay

NCI-H1975 cells were plated in six-well plates (approximately $10^3$ cells per well) in 1 mL of RPMI-1640 medium supplemented with 10% FBS and allowed to adhere overnight. For drug treatment, NPs or TNO155 were added at the specified concentrations the following day, and the medium and compounds were refreshed every 3–4 days. Once the untreated cells reached confluence, colonies were fixed with formaldehyde, stained with 0.2% crystal violet (Sangon Biotech, Shanghai, China), and scanned. For the cell proliferation assay, NCI-H1975 cells (approximately $1.5 \times 10^3$ cells per well) were seeded in 96-well plates and treated with NPs or

TNO155 at concentrations ranging from 0 to 50 μM. On day 3, Cell Counting Kit-8 (CCK-8) reagent (Zoman Biotechnology, Beijing, China) was used. Optical density was measured using a SpectraMax iD5 microplate reader (Molecular Devices, LLC). Untreated wells were used for background correction.

### 2.7. Cell apoptosis assay

NCI-H1975 cells ($1 \times 10^5$ cells per well) were seeded in 12-well plates and cultured in RPMI-1640 medium containing 10% FBS. After 24 h, the cells were treated with 10 μM dihydrotanshinone I (DHT), 10 μM TSA, or 10 μM TNO155. After 24 h of incubation at 37 °C in a 5% $CO_2$ atmosphere, the cells were collected, washed with phosphate-buffered saline (PBS), and resuspended in 150 μL of 1× binding buffer. The samples were then stained with 5 μL of annexin V and 10 μL of propidium iodide (PI) (70-AP107-100; Share-bio Biotechnology, Shanghai, China) at room temperature in the dark for 5 min. Flow cytometric analysis was performed within 1 h using a BD FACSCelesta (Becton, Dickinson and Company, Franklin Lakes, NJ, USA).

### 2.8. Xenograft studies

A suspension ($5 \times 10^6$/mL H1975 cells) was subcutaneously injected into the right flank of five-week-old female BALB/c nude mice. When the average tumor volume reached 50—100 $mm^3$, the mice were randomly assigned to one of three groups. Compounds were formulated in 0.5% sodium carboxymethyl cellulose (CMC-Na) and administered intragastrically at a dose of 20 mg/kg/day. Control mice received an equal volume of 0.5% CMC-Na orally. Body weight and tumor volume were monitored every two days. At the indicated time points, tissue sections were prepared and stained with appropriate antibodies.

### 2.9. Statistics and reproducibility

Quantitative data are expressed as the mean ± standard deviation (SD). Statistical analyses were performed using GraphPad Prism 7.0. A two-sided Student's *t*-test was used to compare the means between two groups.

## 3. Results

### 3.1. Strategy for screening SHP2 inhibitor

An in-house NP library of approximately 1000 molecules was screened using the substrate DiFMUP and a phosphorylated substrate (p-IRS1) as the activator of phosphatase. Full-length SHP2, termed SHP2-FL, was used to identify NPs with enzyme inhibitory potency (at both the active and allosteric sites). Subsequently, catalytic site inhibitors were confirmed by additional screening using SHP2-PTP (truncated form). To further validate the allosteric binding mechanism, the candidate NPs were tested for their biochemical activity against the site-mutated protein $SHP2^{T253M}$. Finally, we employed multiple approaches, including a BLI screening, binding mode simulation, and amino acid mutagenesis, to explore the direct interaction of the active compounds with SHP2 (Fig. 2). This complementary cross-validation protocol led to the identification of SHP2-targeting molecules that bind to the catalytic and allosteric sites.

### 3.2. Protein purification and enzyme assays of SHP2

His-tagged SHP2-FL (M1-L525) and SHP2-PTP (A237-I529) were subsequently purified using HisTrap HP affinity purification, HiTrap Q ion exchange, and HiLoad Superdex200 size-exclusion chromatography. Chromatography and sodium dodecyl sulfate-polyacrylamide gel electrophoresis (SDS-PAGE) results showed the homogeneity of the final purified sample (Figs. 3A and B). The DiFMUP fluorescence assay was used to evaluate the enzymatic activity of the two purified proteins following our previously reported methods [2]. As expected, the results of the enzyme titration experiments showed that SHP2-FL has much weaker catalytic activity than SHP2-PTP, demonstrating that the purified SHP2-FL is tightly regulated and adopts an auto-inhibited conformation (Fig. 3C).

SHP2 is allosterically stimulated by the binding of 2P-IRS-1 to the SH2 domains, which in turn induces the release of the auto-inhibitory conformation, leading to activation of the PTP domain and subsequent preparation of the substrate recognition site for the catalytic reaction. To test this unique characteristic, increasing concentrations of synthetic activating peptide were incubated with SHP2-FL. The dephosphorylating activity of the full-length enzyme gradually increased to a level similar to that of the PTP domain (Fig. 3D). The half maximal effective concentration ($EC_{50}$) value of the 2P-IRS-1 activator for SHP2-FL was 0.354 ± 0.119 μM. Steady-state analysis was performed to evaluate the catalytic kinetics of the surrogate substrate DiFMUP (0—2 mM) toward SHP2-PTP and SHP2-FL in the absence or saturation of the IRS-1 peptide (Fig. 3E). The Michaelis-Menten kinetic parameters shown in Table S1 revealed that fully activated SHP2-FL showed similar $K_M$ value than that of SHP2-PTP (Fig. 3E).

### 3.3. High-throughput screening (HTS) and discovery of SHP2 modulators from NPs

Based on the results of the fluorescence assay with linear enzyme and substrate amount (Figs. 3C—E), 0.5 nM SHP2-FL and 10 μM of DiFMUP were chosen for HTS. The reaction time was set at 0.5 h. To achieve approximate SHP2 protein activation, the concentration of phosphorylated peptide activator was set at 0.5 μM, which was close to the $EC_{50}$ value. The fluorescence signal was read once the substrate was added to eliminate interference from the initial fluorescence of the tested compounds. With the assay conditions set up, a recently reported SHP2 inhibitor from Novartis, TNO155 [10], was used as a condition test to further verify the established SHP2-FL inhibition assay. Consistent with the data reported, TNO155 effectively blocked SHP2-FL activity with a half-maximal inhibitory concentration ($IC_{50}$) value of 34.0 ± 5.4 nM (Fig. 3F).

Using the established assay conditions, we screened and prioritized novel SHP2 inhibitors from our in-house NP library of 976 NPs (Fig. 4A). Based on the SHP2-FL screening, top 40 initial hits that had an inhibition rate of over 60% (at a concentration of 20 μM) were selected. Next, we determined the inhibitory mechanism of active NPs. These initial hits were cross-validated using an SHP2-PTP inhibition assay. NPs that effectively inhibited the catalytic domain were identified as PTP site inhibitors, whereas initial hits with no inhibitory activity toward SHP2-PTP were considered potential allosteric inhibitors. Retesting fresh powders with SHP2-FL and SHP2-PTP revealed 15 confirmed hits with different scaffolds. Representative structures of active SHP2 inhibitors are shown in Fig. 4B. Most of NPs exhibited good activity against SHP2-PTP and SHP2-FL ($IC_{50}$ < 20 μM), among which tanshinon I displayed the strongest inhibitory activity toward PTP domain with $IC_{50}$ value of 3.3 ± 1.2 μM. Interestingly, compound TSA only showed a moderate inhibition activity against SHP2-FL but completely lost activity toward PTP domain, thus acting as a novel allosteric SHP2 inhibitor.

Unlike synthetic compounds, NPs generally have high molecular weights and large chemical scaffolds. In addition, the reported

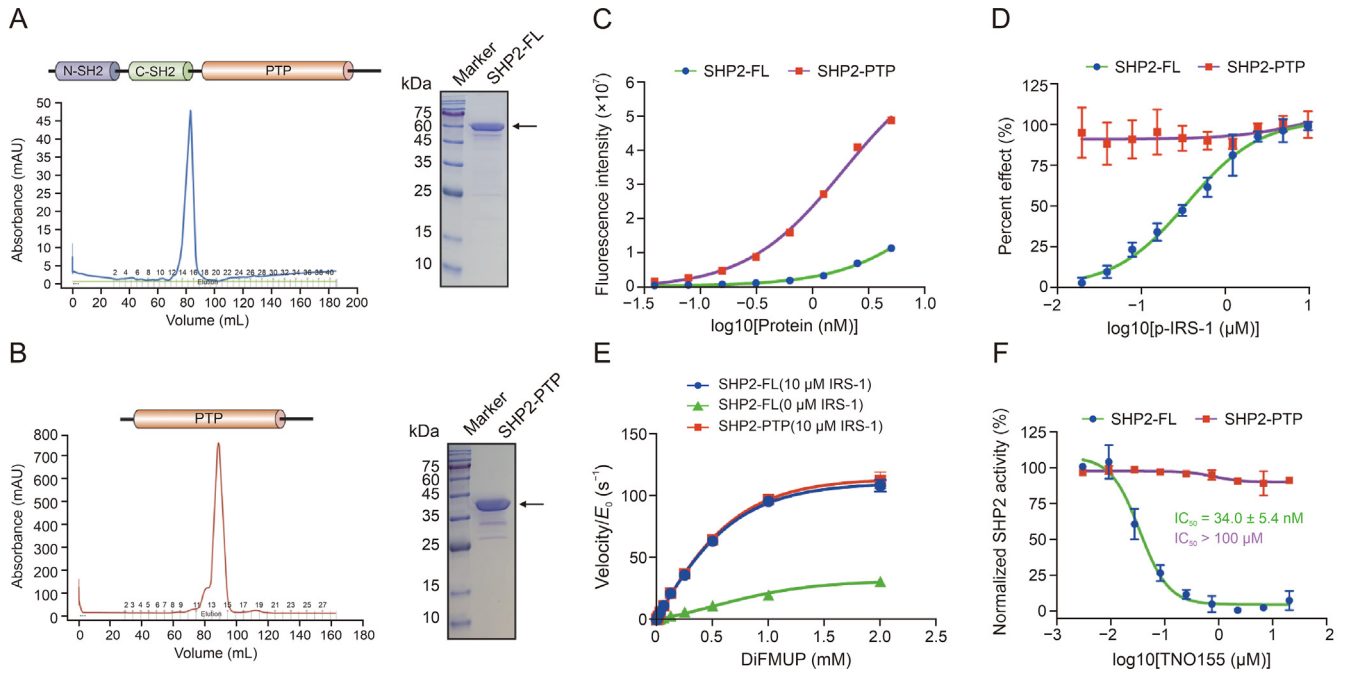


**Fig. 3.** Src homology region 2-containing protein tyrosine phosphatase 2 (SHP2) protein preparation and biochemical activity characterization. (A, B) Representative size-exclusion chromatography of full length SHP2 (SHP2-FL) (M1-L525) (A) and SHP2-protein tyrosine phosphatase (PTP) (A237-I529) (B) proteins. The purities of recombinant human SHP2-FL and SHP2-PTP were evaluated using Coomassie blue stain. The numbers in the *x*-axes of Figs. 3A and B indicate represent the fraction numbers collected during the protein purification process. (C) Enzyme dephosphorylation activity study between full-length and PTP domain of SHP2. (D) Enzymatic activity of enzymes in the presence of 10 μM substrate 6,8-difluoro-4-methylumbellyferyl phosphate (DiFMUP) with the concentration of the synthetic phosphorylated insulin receptor substrate 1 (p-IRS-1) ranging from 0.02 to 10 μM. (E) Enzyme kinetic study of substrate dephosphorylation by enzymes (0.5 nM) at basal or complete activated state. (F) Inhibition effect of TNO155 against SHP2-FL and PTP domain.

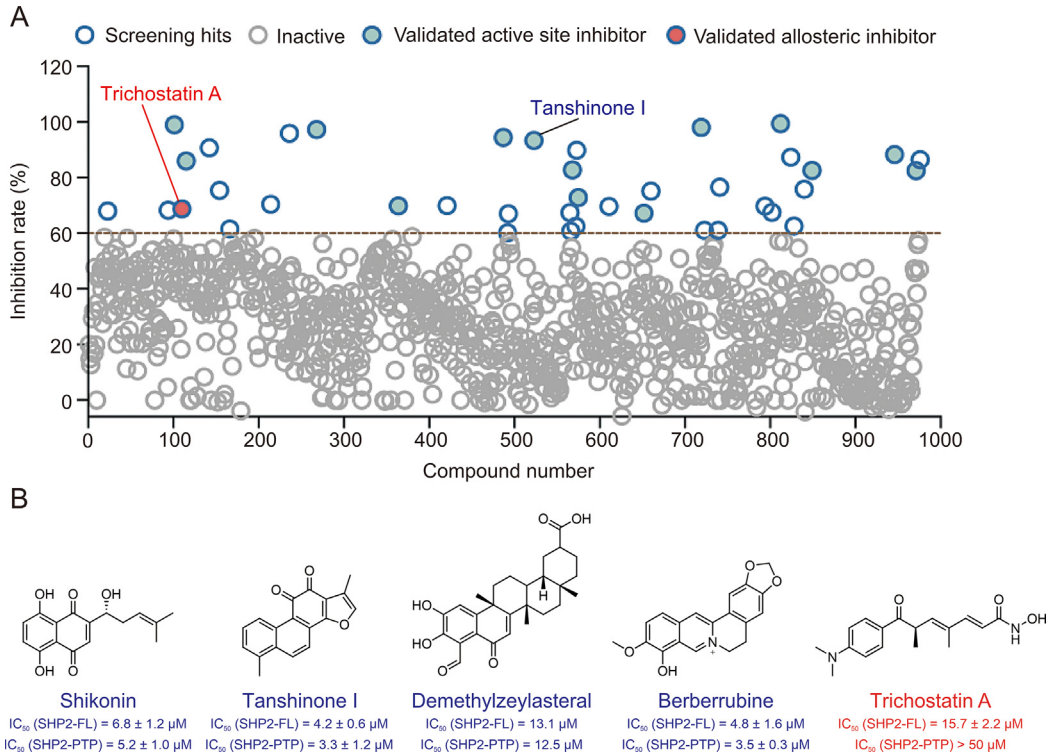


**Fig. 4.** Discovery of Src homology region 2-containing protein tyrosine phosphatase 2 (SHP2) inhibitor from natural products (NPs). (A) First round of screening was performed with a 976-molecule NP library. The line denotes the 60% inhibition rate. The blue and red colored circles denote validated active site and allosteric inhibitors, respectively. Compounds tanshinone I and trichostatin A (TSA) are labeled. (B) Chemical structures and a half-maximal inhibitory concentration ($IC_{50}$) values of screening hits. Data is presented as mean ± standard deviation (SD). $IC_{50}$ values from three experiments on full length SHP2 (SHP2-FL) and SHP2-protein tyrosine phosphatase (PTP) are shown.

allosteric site of SHP2 is significantly smaller than the catalytic site, making NPs more favorable for the PTP domain than allosteric site. Indeed, from the SHP2-FL and SHP2-PTP screening results, the corresponding hit rate was 1.4% (14/976) for SHP-PTP, whereas only one NP was confirmed as an allosteric inhibitor (0.10% hit rate). Based on the primary data from the enzyme assay and the diversity of the structural skeletons with different inhibitory mechanisms, tanshinone derivatives and TSA were selected for further study.

### 3.4. Tanshinone derivatives act as SHP2-PTP inhibitors

Tanshinone derivatives are key bioactive ingredients of the Chinese medicinal herb *Salvia miltiorrhiza* Bunge, which is broadly applied in heart diseases and is the first U.S. Food and Drug Administration (FDA)-approved traditional Chinese medicine in phases II and III clinical trials [30]. Although a series of molecular mechanisms underlying its anticancer and cardioprotective activities have been reported, its direct targets remain unknown [30,31]. A previous study by Liu et al. [22] revealed that the tanshinone derivative cryptotanshinone inhibits SHP2 with an $IC_{50}$ of 22.50 μM. However, the SAR and underlying binding mode of cryptotanshinone remain unclear. These preclinical and clinical studies led us to further investigate the activity of tanshinone derivatives. To explore the preliminary SAR of tanshinones, tanshinone I, tanshinone IIA, DHT, and cryptotanshinone were evaluated for their SHP2-PTP inhibitory activities (Fig. 5A). Interestingly, compounds with reduced furan ring double bonds (DHT and cryptotanshinone) were more favorable for SHP2 inhibition than tanshinones I and IIA. In addition, substitution of the furan ring (sulfonic sodium) significantly decreased SHP2 inhibition activity. Generally, tanshinone I derivatives fused with benzene in ring A are favored over tanshinone IIA derivatives for maintaining enzymatic inhibition activity. The most active compound, DHT, exhibited a well-defined dose-dependent inhibition and suppressed SHP2-PTP dephosphorylation with low $IC_{50}$ values (1.06 ± 0.21 μM), which was 13-fold lower than that of tanshinone IIA (Fig. 5A). DHT showed comparable inhibitory activity against SHP2-FL, indicating that it interfered with the catalytic function of SHP2 (Fig. 5B).

### 3.5. Study on DHT and SHP2-binding sites

To obtain more biochemical evidence to verify the binding site of DHT, molecular docking analysis was conducted, which revealed that DHT located on the SHP2 catalytic cleft blocked the substrate from binding. Specifically, the structural analysis suggested that residues W423 from the WPD loop, R465 from the P-loop, and Q510 from the Q loop formed critical hydrogen bonds with the carboxyl group of the DHT core (Fig. 5C). The furan and benzene ring A moieties formed favorable hydrophobic contacts with the pTyr loop, further stabilizing the occupation of the PTP domain. The

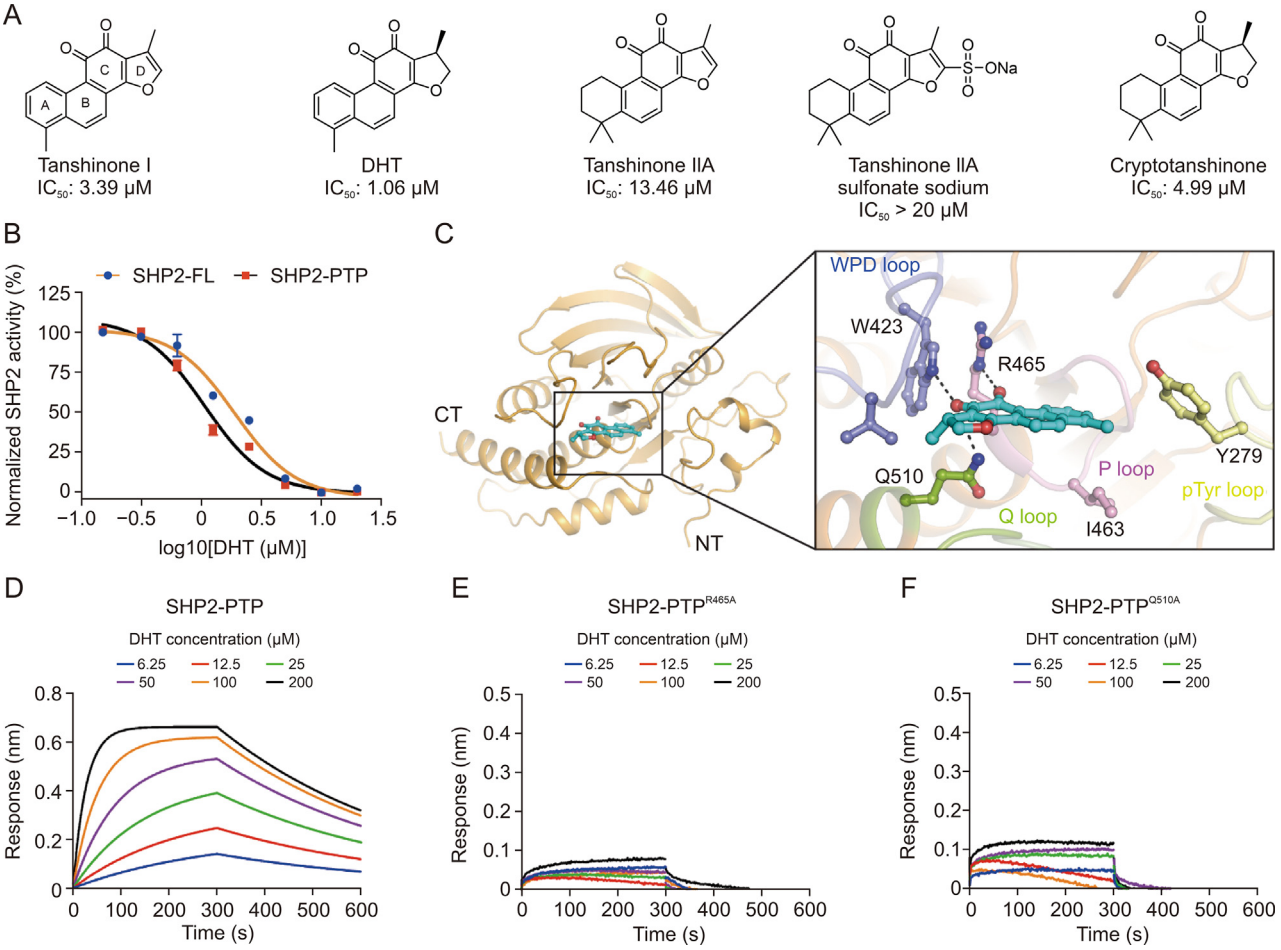


**Fig. 5.** Tanshinone derivatives as inhibitors against Src homology region 2-containing protein tyrosine phosphatase 2 (SHP2)-protein tyrosine phosphatase (PTP). (A) Chemical structures of tanshinones. Half maximal inhibitory concentration ($IC_{50}$) of tanshinones against SHP2-PTP are shown. (B) Inhibition effect of dihydrotanshinone I (DHT) against full length SHP2 (SHP2-FL) or SHP2-PTP. (C) Binding mode of SHP2-PTP and DHT performed in docking studies targeting its catalytic domain. (D–F) Bio-layer interferometry (BLI) assay was used to analyze DHT to SHP2-PTP (D), SHP2-$PTP^{R465A}$ (E), and SHP2-$PTP^{Q510A}$ (F). CT: C terminus; NT: N terminus.

DiFMUP screening results demonstrated that DHT exhibited 4.7-fold higher inhibitory potency against SHP2 than cryptotanshinone. Structural analysis suggested that the aromatic ring A moiety in DHT may engage in enhanced molecular interactions with pTyr and P-loops within the SHP2 catalytic domain through hydrophobic contacts. Next, we performed a BLI experiment to analyze the $K_D$ of DHT in the PTP domain *in vitro*. As shown in Fig. 5D, DHT bound to the PTP domain in a dose-dependent manner ($K_D$ = 396.7 μM). To verify the residues interacting with DHT, two recombinant mutants, SHP2-PTP$^{R465A}$ and SHP2-PTP$^{Q510A}$, were constructed and used in further assays. As shown in Figs. 5E and F, both SHP2-PTP$^{R465A}$ and SHP2-PTP$^{Q510A}$ mutants significantly abolished the direct interaction between DHT and SHP2-PTP *in vitro*. These experimental data helped elucidate the binding mechanism of SHP2-DHT.

### 3.6. Identification of TSA as an allosteric inhibitor of SHP2

Simultaneously, we investigated lead compounds that could utilize the natural autoinhibition mechanism of SHP2 and stabilize it in an inactive state. In a verification experiment using 15 initial hits, we discovered a potential allosteric SHP2 inhibitor, TSA (Fig. 6A). TSA acts as an antifungal antibiotic and inhibitor of histone deacetylase [32]. Recently, there have been reports of the potent inhibition of TSA against sirtuin 6 protein [33]. As shown in Fig. 4A, TSA can inhibit SHP2-FL activity to 68.8% at 20 μM. Furthermore, it dose-dependently inhibited SHP2-FL activity, with an $IC_{50}$ of 15.7 ± 2.2 μM. However, TSA treatment did not affect the enzymatic activity of SHP2-PTP (Fig. 6B).

Based on these *in vitro* results, we investigated the allosteric binding sites of TSA. To date, two verified allosteric sites of SHP2 have been reported, termed allosteric "tunnel" and "latch" [25] (Fig. 6C). First, we predicted the binding poses of TSA within the "tunnel" and "latch" sites using molecular docking, followed by 500 ns MD simulations. Interestingly, our modeling results showed that TSA quickly dissociated from the "latch" binding site of SHP2 and appeared to bind to the "tunnel" binding sites (Video). Therefore, the MD simulation trajectories of TSA bound to "tunnel" binding site of SHP2 were further analyzed. The RMSDs of SHP2 backbone $C_\alpha$ atoms tended to converge after approximately 100 ns of simulations (Fig. 6D). The RMSDs of the TSA heavy atoms converged after approximately 150–270 ns in the MD simulations (Fig. 6E).

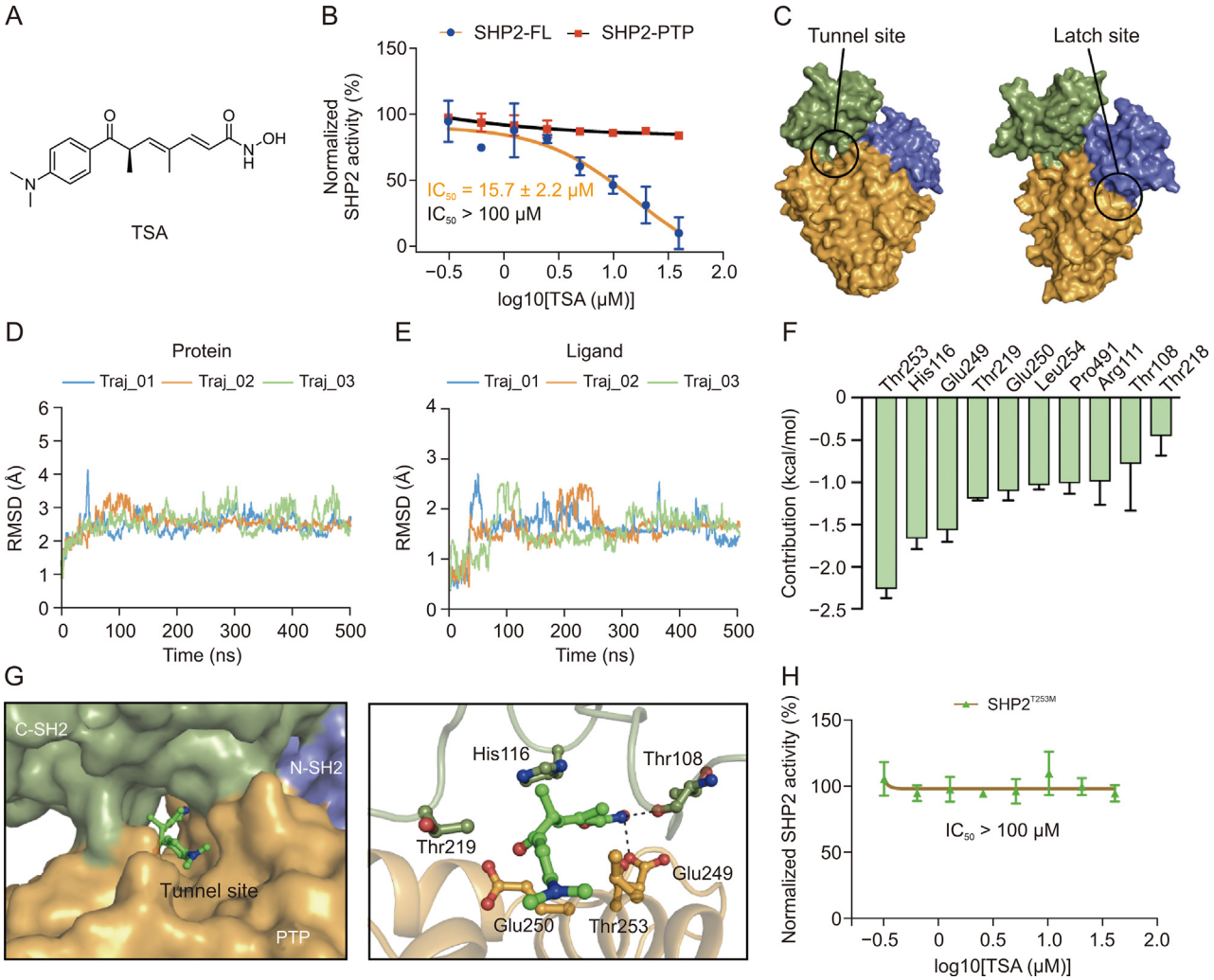


**Fig. 6.** Identification of trichostatin A (TSA) as a Src homology region 2-containing protein tyrosine phosphatase 2 (SHP2) allosteric site inhibitor. (A) Structures of TSA. (B) Effect of TSA on the dephosphorylation activity of the full length SHP2 (SHP2-FL) (orange line) or catalytic domain (black line). (C) Tunnel and latch sites of SHP2. (D) The root mean square deviations (RMSDs) of the protein backbone $C_\alpha$ atoms of SHP2 tended to converge after approximately 100 ns of MD simulations. (E) The RMSDs of TSA heavy atoms after approximately 150–270 ns of MD simulations. (F) Predicted crucial residues mediated SHP2-TSA interaction. (G) Molecular modeling of TSA bound to the SHP2 tunnel site. (H) TSA had a significantly compromised activity against SHP2$^{T253M}$ mutants. PTP: protein tyrosine phosphatase; $IC_{50}$: half-maximal inhibitory concentration; Traj: trajectory.

**Table 1**
Selectivity profiling of dihydrotanshinone I (DHT) and trichostatin A (TSA) in selected phosphatase enzyme panel.

| Phosphatase | Species | Class | Sequence of recombinant protein | $IC_{50}$ (mM) | |
|---|---|---|---|---|---|
| | | | | DHT | TSA |
| PTPN1 (PTP1B) | Human | Classic non-receptor PTPs (class I) | M1-N321 | 9.3 ± 0.94 | >100 |
| PTPN6 (SHP1) | Human | Classic non-receptor PTPs (class I) | M1-K591 | 2.5 ± 0.3 | >100 |
| PTPN12 (PTP-PEST) | Human | Classic non-receptor PTPs (class I) | M1-G305 | 32.1 ± 3.8 | >100 |
| PTPRA (RPTPα) | Human | Classic receptor PTPs (class I) | A174-K793 | 50.4 ± 5.3 | >100 |
| LMWPTP (ACP1) | Human | Class II | M1-H158 | >100 | >100 |

$IC_{50}$: half-maximal inhibitory concentration; PTPN1: protein tyrosine phosphatase (PTP) non-receptor type 1; PTP1B: protein tyrosine phosphatase 1B; SHP1: Src homology region 2-containing protein tyrosine phosphatase 1; PEST: PTP containing a PEST motif (rich in Pro, Glu, Ser, and Thr); PTPRA: protein tyrosine phosphatase receptor type A; RPTPα: receptor-like PTP alpha; LMWPTP: low molecular weight PTP; ACP1: acid phosphatase locus 1.

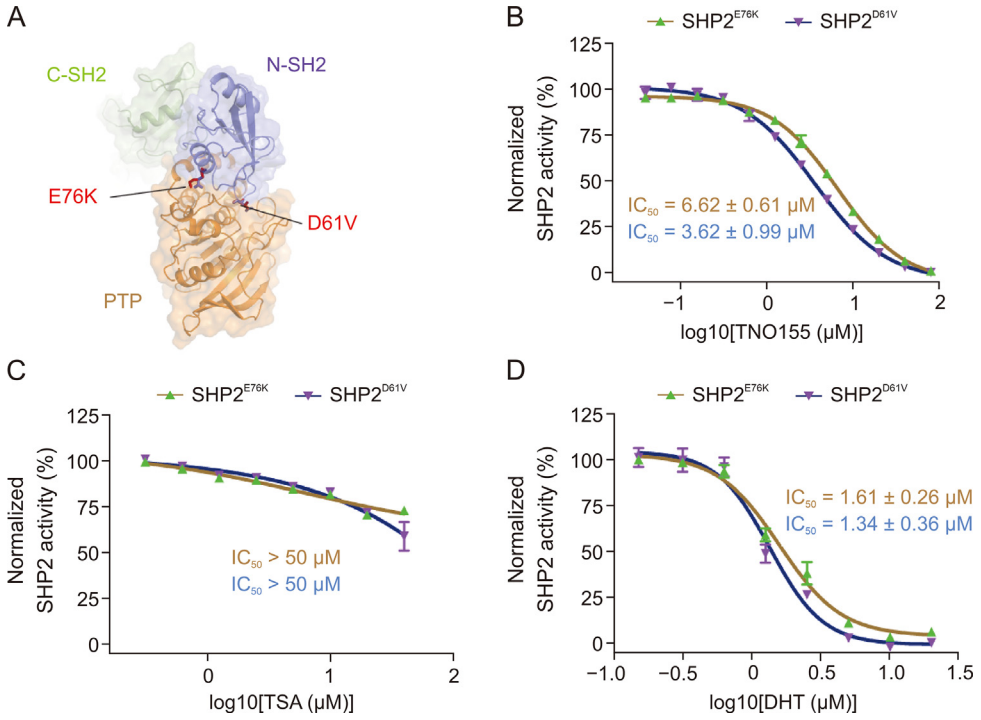


**Fig. 7.** Active natural products (NPs) against Src homology region 2-containing protein tyrosine phosphatase 2 (SHP2) oncogenic mutations. (A) Sites of E76K and D61V activating alterations of SHP2 mapped on its SH2-protein tyrosine phosphatase (PTP) interface (Protein Data Bank (PDB) ID: 2SHP). The E76K and D61V mutations are shown in red. (B–D) $SHP2^{E76K}$ and $SHP2^{D61V}$ inhibition by TNO155 (B), trichostatin A (TSA) (C), and dihydrotanshinone I (DHT) (D) with various compound concentrations. $IC_{50}$: half maximal inhibitory concentration.

Those results indicate the TSA possibly bound to "tunnel" site of SHP2. The dynamic co-structures of the SHP2/TSA binary complexes were then subjected to per-residue decomposition using the MM/GBSA method. Residues Thr253, His116, Glu249, Thr219, Glu250, Leu254, Pro491, Arg111, Thr108, and Thr218 were predicted to be critical for SHP2-TSA interaction (Fig. 6F). Structural analysis revealed that residues Thr108 and Glu249 played significant roles in the interactions by forming critical hydrogen bonds with TSA (Fig. 6G).

In search of more biochemical evidence of "tunnel" site interaction, an engineered $SHP2^{T253M}$ protein with mutation in the allosteric pocket was used in the following study, which prevented inhibitors from binding to the "tunnel" site (Fig. S1A). $SHP2^{T253M}$ retained its autoinhibitory features and catalytic activity in the p-IRS-1 titration assay. However, TSA showed 100-fold less potency against $SHP2^{T253M}$ cells than the wild-type enzyme (Figs. 6H and S1B). Notably, Thr253 was predicted to contribute the most to the binding of TSA to SHP2 (Fig. 6F). Additionally, the engineered $SHP2^{T253M}$ mutation eliminated the efficacy of TNO155, further confirming the allosteric mechanisms of TNO155 and TSA (Fig. S1C). Therefore, we provide a new mechanism for the antitumor effect of TSA, which functions as a "glue" to make the closed form of SHP2 more stabilized. Although the inhibitory ability of TSA is moderate, further structural modifications may lead to the discovery of more potent allosteric small molecule inhibitors. While TSA is a previously reported HDAC inhibitor, our findings suggest its potential as a foundation for developing dual-target SHP2/HDAC inhibitors.

### 3.7. Preliminary selectivity of DHT and TSA against PTPs

Similar to the kinase domain of RTKs, the catalytic domain of PTPs is relatively conserved. Therefore, it is challenging to discover highly selective SHP2 inhibitors. To determine the functional specificities of DHT and TSA, their inhibitory activities were evaluated against a panel of selected PTPs: PTPRA (receptor type), PTPN1 and PTPN12 (non-receptor type), and LMWPTP (class II PTP). DHT inhibited the PTP (PTPN1, PTPN12, and PTPRA)-catalyzed hydrolysis of DiFMUP with an $IC_{50}$ of 9.3 ± 0.94, 32.1 ± 3.8, and 50.4 ± 5.3 μM, respectively, which was approximately 8-fold to 47-fold less active than SHP2. The $IC_{50}$ of DHT against LMW-PTP was more than 100 μM (Table 1). As the catalytic region of SHP2 is almost identical to that of SHP1 (PTPN6) [34], DHT showed high inhibitory activity against

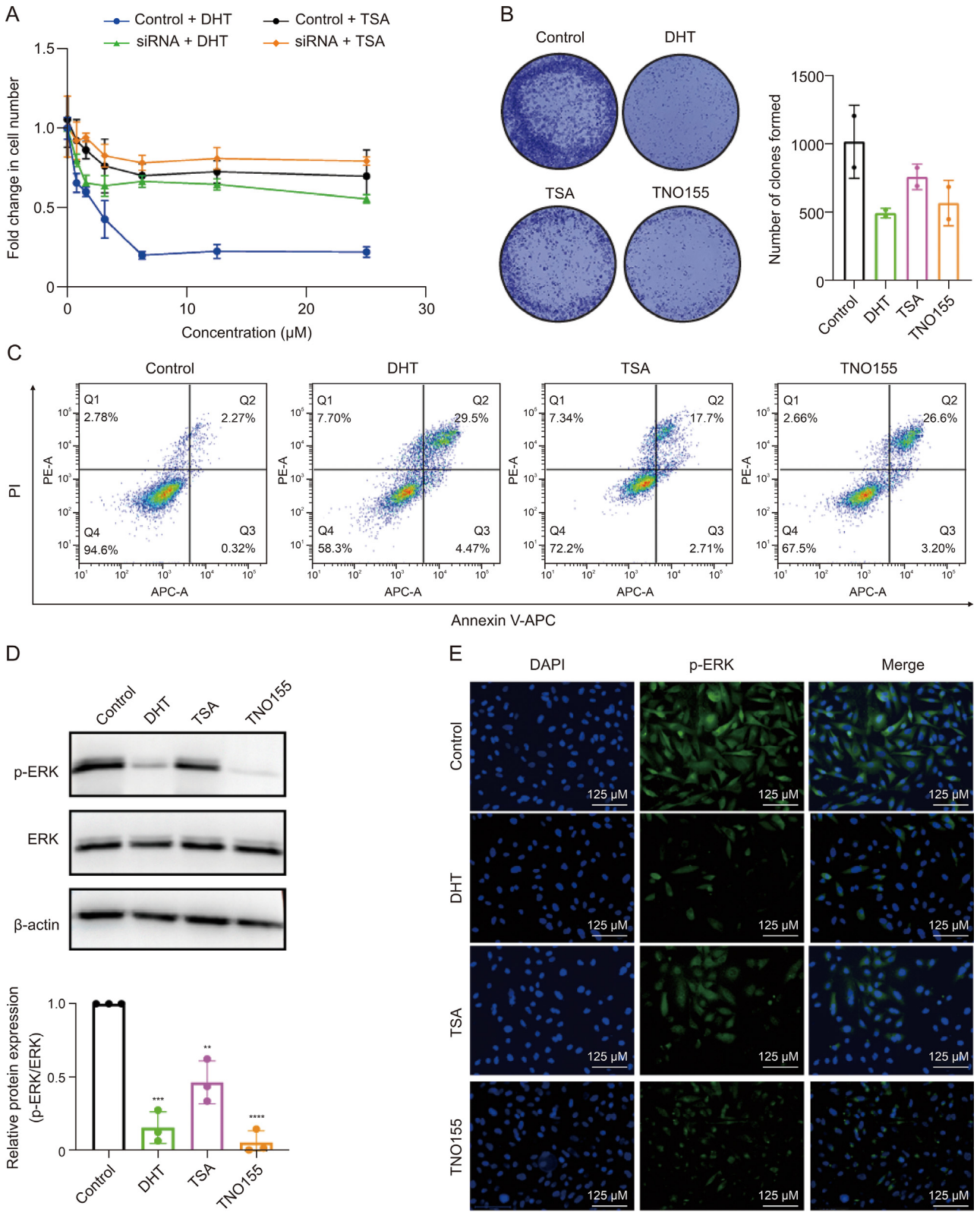


**Fig. 8.** Active natural products (NPs) inhibited Src homology region 2-containing protein tyrosine phosphatase 2 (SHP2)-mediated signaling in H1975 cells. (A) Anti-proliferation effects of dihydrotanshinone I (DHT) and trichostatin A (TSA) were decreased in SHP2 small interfering RNA (siRNA) treated H1975 cells. (B) Colony formation of H1975 after DHT, TSA, and TNO155 treatment. Colony formation was measured 10 days after compound treatment. (C) Apoptosis analysis of H1975 cells after treating with 10 μM DHT, TSA, or TNO155 for 24 h. (D) Analyses of phosphorylated extracellular signal-regulated kinase (p-ERK), ERK, and β-actin from H1975 cells supplemented with 10 μM DHT, TSA, and TNO155. (E) 4′,6-Diamidino-2-phenylindole (DAPI) and p-ERK stainings for H1975 cells treated with DMSO or 10 μM DHT, TSA, or TNO155. PI: propidium iodide; PE-A: R-phycoerythrin; APC: allophycocyanin.

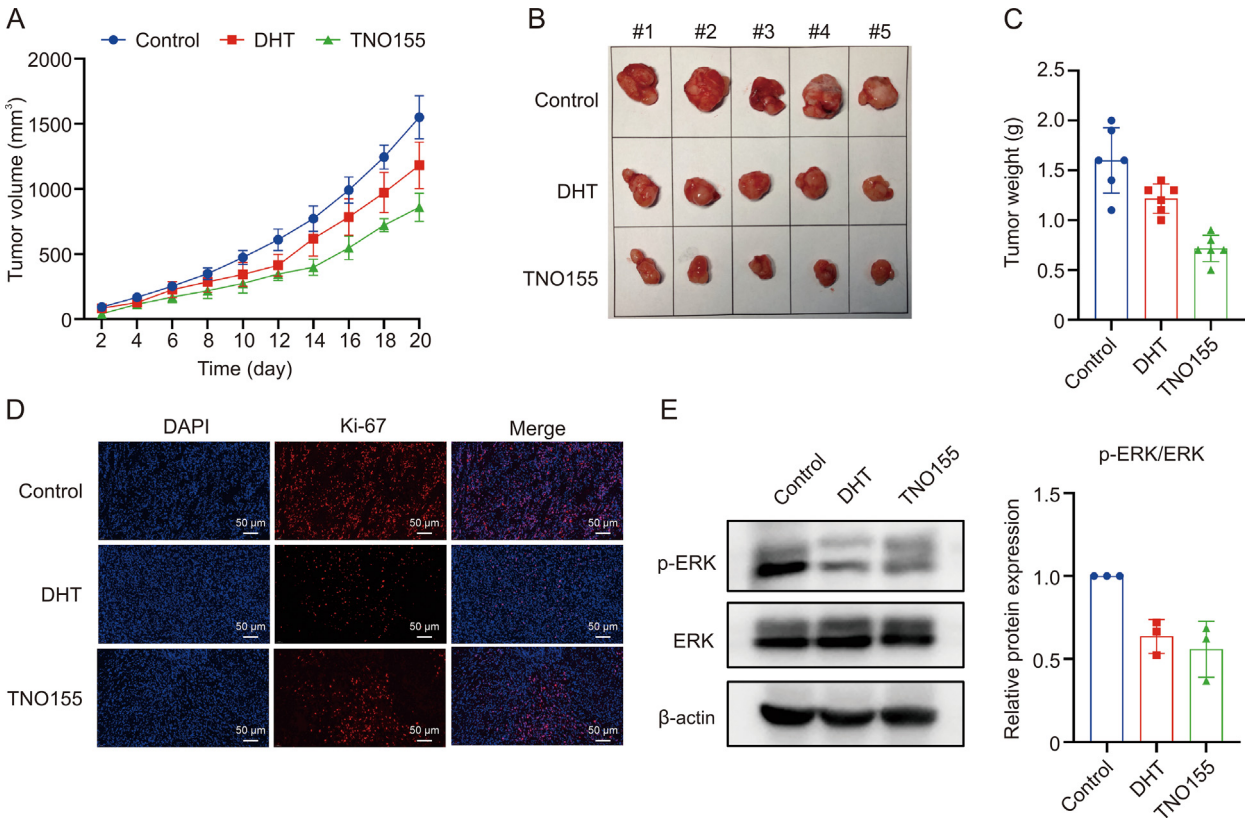


**Fig. 9.** Evaluation of dihydrotanshinone I (DHT) in epidermal growth factor receptor (EGFR)-driven cancer *in vivo*. (A) Antitumor efficacy evaluation of DHT and TNO155 in the H1975 xenograft mouse model. (B) Representative images of tumors in each group after vehicle, DHT, or TNO155 treatment. (C) Tumor weights in each group after treatment with DHT and TNO155. (D) Ki-67 staining in tumor tissues. (E) Measurement of phosphorylated extracellular signal-regulated kinase (p-ERK) levels in tumor lysates via Western blot (left) and the corresponding statistical analysis (right). DAPI: 4′,6-diamidino-2-phenylindole.

SHP1, with an $IC_{50}$ of 2.5 ± 0.3 μM. A previous study demonstrated that DHT derivatives potently inhibit SHP1 because of the high homology of the catalytic sites between SHP2 and SHP1 [22]. Nevertheless, DHT is still valuable for the treatment of SHP2-related diseases because SHP2 is ubiquitously expressed, whereas SHP1 is normally expressed only in hematopoietic cells. In contrast, TSA showed no detectable inhibitory activity against any of the three types of PTPs, likely because of the particularity of the SHP2 tunnel site among the PTPs. These preliminary data show that DHT and TSA have a certain selectivity for the PTP family, but the selectivity for the entire PTP family needs further verification.

### 3.8. Active NPs against SHP2 oncogenic mutations

Activating mutations in SHP2 cause solid tumors and hematological cancers and occur frequently in Noonan syndrome [10]. Herein, we investigated the effects of oncogenic mutations on the inhibitory effects of TNO155 and active NPs using biochemical assays. The two most frequently occurring SHP2 variants bearing oncogenic mutations (E76K and D61V) were previously found to induce domain reorganization and expose catalytic sites (Fig. 7A). Site-directed mutagenesis was used to create the constructs $SHP2^{E76K}$ and $SHP2^{D61V}$, which were expressed and purified in a manner similar to that of SHP2-FL (Fig. S2A). Indeed, a large increase in the catalytic activity of the substrate was observed without p-IRS-1, confirming the changes in the autoinhibition conformation (Fig. S2B).

To further investigate how these gain-of-function mutations affected the inhibition of SHP2 phosphatase by the active compounds, we titrated TNO155, TSA, and DHT against SHP2 and measured the dephosphorylation activity of different enzymes. In the basal state, the E76K and D61V mutations reduced the activity of TNO155 *in vitro*. The potency decreased by more than 60-fold in the $SHP2^{E76K}$ and $SHP2^{D61V}$ mutants compared to that in SHP2-FL (Fig. 7B). The allosteric inhibitor TSA showed a similar trend in response to the SHP2 cancer mutants (Fig. 7C). In contrast, both activating enzymes were strongly inhibited by DHT, with $IC_{50}$ values of 1.61 ± 0.26 to 1.34 ± 0.36 μM, respectively (Fig. 7D). Based on the structural basis and binding modes, the efficacy of allosteric inhibition by TSA is antagonized by the E76K and D61V gain-of-mutations. In contrast, the SHP2 PTP domain inhibitor, DHT, which interacts with the catalytic site, has potential implications for SHP2 oncoproteins that are resistant to allosteric inhibitors. The simultaneous occupation of both active and allosteric sites by DHT along with TNO155 is feasible in cases of SHP2 oncogenic mutation-induced cancer or Noonan syndrome.

### 3.9. Evaluation of SHP2 inhibitors in RTK-driven non-small cell lung cancer (NSCLC)

Earlier studies have shown that most RTK-driven cancer cells depend on SHP2 catalytic activity of for proliferation. It has been established that SHP2 inhibitors reduce the viability of malignancies driven by RTK by inhibiting MAPK signaling [2]. To validate the anticancer potency and mechanism of action of these SHP2 inhibitors, DHT and TSA were used to treat RTK-driven cancers. The NCI-H1975 cell line was used in the following study because of its distinct epidermal growth factor receptor (EGFR) alterations and proliferation of this NSCLC cell, which has been reported to rely on SHP2. As shown in Figs. 8A and B, treatment with DHT and TSA

resulted in a significant suppression of proliferation and colony formation in NCI-H1975 cells. To validate that the mechanism of antiproliferation effects of DHT and TSA, we also tested the active compounds in SHP2 knockdown H1975 cells (Fig. S3). As shown in Fig. 8A, SHP2 was the primary target, as evidenced by the significantly lower sensitivity of SHP2-depleted H1975 cells to DHT and TSA. Consistently, the two active compounds dramatically increased apoptotic cell death in NCI-H1975 cells (Fig. 8C).

Next, we evaluated the effects of DHT and TSA on SHP2 signaling using the phosphorylation levels of ERK as a readout. As shown in Fig. 8D, untreated cancer cells retained considerable levels of ERK phosphorylation. In contrast, there was a significant decrease in ERK phosphorylation after treatment with DHT and TSA. In addition, treatment with both compounds weakened the immunofluorescence signal of p-ERK, demonstrating that the active compounds efficiently inhibited the MAPK signaling pathway via SHP2 blockage (Fig. 8E).

The *in vivo* efficacy of DHT in the NCI-H1975 xenograft model was subsequently evaluated based on its potent antiproliferative activity in NCI-H1975 cells. The mice were administered DHT or TNO155 via oral gavage at a daily dose of 20 mg/kg. DHT administration resulted in significant tumor growth suppression after a 20-day treatment compared to that in the vehicle group (Figs. 9A–C). No body weight loss was observed over the full treatment course, indicating that DHT was well tolerated (Fig. S4). Moreover, DHT treatment resulted in a marked decrease in MAPK phosphorylation and cancer cell proliferation activity with reduced Ki-67 staining positive areas in tumor tissue compared to the vehicle group (Figs. 9D and E). Thus, DHT is a potential therapeutic agent for the treatment of RTK-dependent malignancies.

## 4. Discussion

Phosphorylation of tyrosine residues is mediated by a balance via the cooperation of RTKs and PTPs. Therefore, PTPs are recognized as crucial regulators. The PTP superfamily currently has over 100 members that are being explored as therapeutic drug targets for various diseases, including tumors, autoimmunity, and metabolic and cardiovascular diseases. To date, approximately 30 drugs approved by the FDA target tyrosine kinases; however, PTP-targeted drug development remains challenging. *PTPN11* is a unique member of the PTP family that participates in various signaling pathways, including PI3K, MAPK, and PD-L1 signaling. SHP2 is a promising target for cancer and other developmental diseases [35,36]. Despite 20 years of investigation on the fundamental role of SHP2 in oncogenic and developmental diseases, only a few allosteric inhibitors or degraders [37] have advanced into the early clinical stage. Given its clinical importance and current drug development paradigm, the development of novel inhibitors or degraders of SHP2 for cancer therapy is urgently needed.

In this study, 15 NPs were validated as hit compounds from the NP library with approximately 1000 compounds. Among these active NPs, tanshinone derivatives have been validated as catalytic-site inhibitors of SHP2. Further preliminary SAR analysis led to the identification of DHT as an SHP2 inhibitor with improved activity among a series of analogs. We next applied DiFMUP and BLI assays in conjunction with molecular simulation and site-directed mutation studies to confirm that DHT functions by binding to the active site of SHP2. Site-directed mutagenesis experiments supported the docking studies and provided a structural rationale for DHT-SHP2 binding. SHP2 inhibition by DHT significantly inhibited the proliferation of EGFR-driven cancer cells. In addition, DHT showed 8–47-fold selectivity for PTP1B, PTPN12, PTPRA, and LMWPTP from different classes of PTPs. Further medicinal chemistry studies on DHT are necessary to establish more defined SAR data and optimize it to a lower $IC_{50}$ value and better SHP2 selectivity. Our study provides a potential drug target for tanshinone analogs for preclinical and clinical studies.

In addition to NPs inhibiting the SHP2 PTP domain, another interesting small-molecule compound, TSA, was identified as an inhibitor that stabilized the inactive conformation. Similar to TNO155, activating mutations weakened the inhibitory effects of TSA on SHP2. Using MD analysis, we studied the molecular mechanism of TSA by inserting it into the same allosteric tunnel site as that of TNO155. The tunnel site-blocked SHP2 variant ($SHP2^{T253M}$) significantly diminished TSA activity. Although TSA exhibited a relatively high $IC_{50}$ of 15.7 μM, it exhibited good selectivity over other PTPs due to the unique allosteric site in SHP2. The cocrystallization of TSA and SHP2-FL should be investigated to uncover the underlying molecular basis.

Mutations, such as E76K and D61V, commonly occur in patients with Noonan syndrome [38]. A recent study revealed that SHP2 variants can recruit normal SHP2 to phase-separated condensates, thereby stimulating downstream signaling [39]. As the drug-binding pocket of SHP2 is only available in its auto-inhibited state, the currently reported allosteric inhibitors are ineffective against these SHP2 oncogenic gain-of-function mutations [40]. It is interesting that DHT robustly inhibits both the activating forms of SHP2 with a much lower $IC_{50}$ than TNO155. Therefore, we speculate that DHT can be used in combination with allosteric inhibitors for mutant SHP2-related diseases through the simultaneous inhibition of both active and allosteric sites. As DHT exhibits a modest antitumor effect *in vivo*, further structural modifications of DHT are necessary to improve its potency or pharmacokinetic properties.

## 5. Conclusion

In summary, we developed an HTS assay strategy for screening NPs and identified lead compounds with structurally diverse scaffolds. Biochemical and cell-based results provide evidence of the binding modes, and targeting SHP2 is a feasible strategy for treating cancers with RTK overexpression. These active compounds serve as new probes for studying the function of SHP2 in tumorigenesis and immune checkpoint modulation and development. Further structural modifications, discovery of SHP2 selective inhibitors, and investigation of these SHP2-binding NPs in other SHP2-related inflammatory diseases, such as colitis and diabetes, should be performed.

## CRediT authorship contribution statement

**Lingfeng Chen:** Writing – original draft, Investigation, Funding acquisition, Data curation, Conceptualization. **Di Ke:** Data curation. **Zheng Jiang:** Writing – review & editing, Investigation. **Ruixiang Luo:** Methodology, Investigation, Data curation. **Jie Li:** Investigation. **Lulu Zheng:** Validation, Investigation. **Guang Liang:** Writing – review & editing, Supervision, Funding acquisition, Conceptualization.

## Declaration of competing interest

The authors declare that they have no known competing financial interests or personal relationships that could have appeared to influence the work reported in this paper.

## Acknowledgments

This work was supported by the National Natural Science Foundation of China (Grant Nos.: 82422068 and U24A20814), the Natural Science Funding of Zhejiang Province, China (Grant Nos.:

LDG25H300001 and LR24H300001). The authors acknowledge the support from the Scientific Research Center, Hangzhou Medical College.

## Appendix A. Supplementary data

Supplementary data to this article can be found online at https://doi.org/10.1016/j.jpha.2025.101335.

## References

[1] R.J. Chan, G. Feng, PTPN11 is the first identified proto-oncogene that encodes a tyrosine phosphatase, Blood 109 (2007) 862–867.
[2] Y.P. Chen, M.J. LaMarche, H.M. Chan, et al., Allosteric inhibition of SHP2 phosphatase inhibits cancers driven by receptor tyrosine kinases, Nature 535 (2016) 148–152.
[3] T. Okazaki, S. Chikuma, Y. Iwai, et al., A rheostat for immune responses: The unique properties of PD-1 and their advantages for clinical application, Nat. Immunol. 14 (2013) 1212–1218.
[4] Z. Guo, Y. Duan, K. Sun, et al., Advances in SHP2 tunnel allosteric inhibitors and bifunctional molecules, Eur. J. Med. Chem. 275 (2024), 116579.
[5] P. Hof, S. Pluskey, S. Dhe-Paganon, et al., Crystal structure of the tyrosine phosphatase SHP-2, Cell 92 (1998) 441–450.
[6] J.R. LaRochelle, M. Fodor, V. Vemulapalli, et al., Structural reorganization of SHP2 by oncogenic mutations and implications for oncoprotein resistance to allosteric inhibition, Nat. Commun. 9 (2018), 4508.
[7] L. Chen, S.S. Sung, M.L. Richard Yip, et al., Discovery of a novel Shp2 protein tyrosine phosphatase inhibitor, Mol. Pharmacol. 70 (2006) 562–570.
[8] K. Hellmuth, S. Grosskopf, C.T. Lum, et al., Specific inhibitors of the protein tyrosine phosphatase Shp2 identified by high-throughput docking, Proc. Natl. Acad. Sci. U S A 105 (2008) 7275–7280.
[9] X. Yuan, H. Bu, J. Zhou, et al., Recent advances of SHP2 inhibitors in cancer therapy: Current development and clinical application, J. Med. Chem. 63 (2020) 11368–11396.
[10] M.J. LaMarche, M. Acker, A. Argintaru, et al., Identification of TNO155, an allosteric SHP2 inhibitor for the treatment of cancer, J. Med. Chem. 63 (2020) 13578–13594.
[11] D. Shen, W. Chen, J. Zhu, et al., Therapeutic potential of targeting SHP2 in human developmental disorders and cancers, Eur. J. Med. Chem. 190 (2020), 112117.
[12] A.M. Taylor, B.R. Williams, F. Giordanetto, et al., Identification of GDC-1971 (RLY-1971), a SHP2 inhibitor designed for the treatment of solid tumors, J. Med. Chem. 66 (2023) 13384–13399.
[13] A. Drilon, M.R. Sharma, M.L. Johnson, et al., SHP2 inhibition sensitizes diverse oncogene-addicted solid tumors to re-treatment with targeted therapy, Cancer Discov. 13 (2023) 1789–1801.
[14] I. Brana, G. Shapiro, M.L. Johnson, et al., Initial results from a dose finding study of TNO155, a SHP2 inhibitor, in adults with advanced solid tumors, J. Clin. Oncol. 39 (2021), 3005.
[15] A.G. Atanasov, S.B. Zotchev, V.M. Dirsch, et al., Natural products in drug discovery: Advances and opportunities, Nat. Rev. Drug Discov. 20 (2021) 200–216.
[16] D.J. Newman, G.M. Cragg, Natural products as sources of new drugs over the nearly four decades from 01/1981 to 09/2019, J. Nat. Prod. 83 (2020) 770–803.
[17] J. Lu, D. Yu, H. Li, et al., Promising natural products targeting protein tyrosine phosphatase SHP2 for cancer therapy, Phytother. Res. 39 (2025) 1735–1757.
[18] C. Jiang, L. Liang, Y. Guo, Natural products possessing protein tyrosine phosphatase 1B (PTP1B) inhibitory activity found in the last decades, Acta Pharmacol. Sin. 33 (2012) 1217–1245.
[19] T.O. Johnson, J. Ermolieff, M.R. Jirousek, Protein tyrosine phosphatase 1B inhibitors for diabetes, Nat. Rev. Drug Discov. 1 (2002) 696–709.
[20] L.M. Scott, L. Chen, K.G. Daniel, et al., Shp2 protein tyrosine phosphatase inhibitor activity of estramustine phosphate and its triterpenoid analogs, Bioorg. Med. Chem. Lett. 21 (2011) 730–733.
[21] S. Liu, Z. Yu, X. Yu, et al., SHP2 is a target of the immunosuppressant tautomycetin, Chem. Biol. 18 (2011) 101–110.
[22] W. Liu, B. Yu, G. Xu, et al., Identification of cryptotanshinone as an inhibitor of oncogenic protein tyrosine phosphatase SHP2 (*PTPN11*), J. Med. Chem. 56 (2013) 7212–7221.
[23] Y. Song, M. Zhao, Y. Wu, et al., A multifunctional cross-validation high-throughput screening protocol enabling the discovery of new SHP2 inhibitors, Acta Pharm. Sin. B 11 (2021) 750–762.
[24] R.J. Nichols, F. Haderk, C. Stahlhut, et al., RAS nucleotide cycling underlies the SHP2 phosphatase dependence of mutant BRAF-, NF1- and RAS-driven cancers, Nat. Cell Biol. 20 (2018) 1064–1073.
[25] M. Fodor, E. Price, P. Wang, et al., Dual allosteric inhibition of SHP2 phosphatase, ACS Chem. Biol. 13 (2018) 647–656.
[26] W. Fu, M. Zhang, J. Liao, et al., Discovery of a novel androgen receptor antagonist manifesting evidence to disrupt the dimerization of the ligand-binding domain via attenuating the hydrogen-bonding network between the two monomers, J. Med. Chem. 64 (2021) 17221–17238.
[27] W. Fu, E. Wang, D. Ke, et al., Discovery of a novel *Fusarium graminearum* mitogen-activated protein kinase (FgGpmk1) inhibitor for the treatment of *Fusarium* head blight, J. Med. Chem. 64 (2021) 13841–13852.
[28] D.R. Roe, T.E. Cheatham 3rd, PTRAJ and CPPTRAJ: Software for processing and analysis of molecular dynamics trajectory data, J. Chem. Theor. Comput. 9 (2013) 3084–3095.
[29] W. Zhou, M. Duan, W. Fu, et al., Discovery of novel androgen receptor ligands by structure-based virtual screening and bioassays, Genom. Proteom. Bioinform. 16 (2018) 416–427.
[30] S. Xu, P. Liu, Tanshinone II-A: New perspectives for old remedies, Expert Opin. Ther. Pat. 23 (2013) 149–153.
[31] S. Gao, Z. Liu, H. Li, et al., Cardiovascular actions and therapeutic potential of tanshinone IIA, Atherosclerosis 220 (2012) 3–10.
[32] D.C. Drummond, C.O. Noble, D.B. Kirpotin, et al., Clinical development of histone deacetylase inhibitors as anticancer agents, Annu. Rev. Pharmacol. Toxicol. 45 (2005) 495–528.
[33] W. You, C. Steegborn, Structural basis of sirtuin 6 inhibition by the hydroxamate trichostatin A: Implications for protein deacylase drug development, J. Med. Chem. 61 (2018) 10922–10928.
[34] X. Xu, T. Masubuchi, Q. Cai, et al., Molecular features underlying differential SHP1/SHP2 binding of immune checkpoint receptors, Elife 10 (2021), e74276.
[35] Z. Song, M. Wang, Y. Ge, et al., Tyrosine phosphatase SHP2 inhibitors in tumor-targeted therapies, Acta Pharm. Sin. B 11 (2021) 13–29.
[36] N.M. Sodir, G. Pathria, J.I. Adamkewicz, et al., SHP2: A pleiotropic target at the interface of cancer and its microenvironment, Cancer Discov. 13 (2023) 2339–2355.
[37] M. Wang, J. Lu, M. Wang, et al., Discovery of SHP2-D26 as a first, potent, and effective PROTAC degrader of SHP2 protein, J. Med. Chem. 63 (2020) 7510–7528.
[38] J.P. Vainonen, M. Momeny, J. Westermarck, Druggable cancer phosphatases, Sci. Transl. Med. 13 (2021), eabe2967.
[39] G. Zhu, J. Xie, W. Kong, et al., Phase separation of disease-associated SHP2 mutants underlies MAPK hyperactivation, Cell 183 (2020) 490–502.e18.
[40] R.A.P. Pádua, Y. Sun, I. Marko, et al., Mechanism of activating mutations and allosteric drug inhibition of the phosphatase SHP2, Nat. Commun. 9 (2018), 4507.